JOURNAL OF VIROLOGY, Aug. 1995, p. 5095–5102 Vol. 69, No. 8
0022-538X/95/$04.00+0

Retroviral Integration at the *Evi-2* Locus in BXH-2 Myeloid Leukemia Cell Lines Disrupts *Nf1* Expression without Changes in Steady-State Ras-GTP Levels

DAVID A. LARGAESPADA, JOHN D. SHAUGHNESSY, JR., NANCY A. JENKINS, AND NEAL G. COPELAND*

Mammalian Genetics Laboratory, ABL-Basic Research Program, NCI-Frederick Cancer Research and Development Center, Frederick, Maryland 21702

Received 28 February 1995/Accepted 10 May 1995

Approximately 15% of BXH-2 myeloid leukemias harbor proviral integrations at the *Evi-2* common viral integration site. *Evi-2* is located within a large intron of the *Nf1* tumor suppressor gene, raising the possibility that proviral integration at *Evi-2* predisposes mice to myeloid tumor development by disrupting *Nf1* expression. This hypothesis is supported by data suggesting that mutations in the human *NF1* gene are causally associated with the development of juvenile chronic myelogenous leukemia (K. M. Shannon, P. O'Connell, G. A. Martin, D. Paderanga, K. Olson, P. Dinndorf, and F. McCormick, N. Engl. J. Med. 330:597–601, 1994) and mouse studies showing that aged mice, heterozygous for a germ line *Nf1* mutation, develop myeloid leukemia with loss of the wild-type *Nf1* allele (T. Jacks, T. S. Shih, E. M. Schmitt, R. T. Bronson, A. Bernards, and R. A. Weinberg, Nat. Genet. 7:353–361, 1994). To determine if viral integration at *Evi-2* disrupts *Nf1* expression, we derived a series of BXH-2 myeloid leukemia cell lines with or without viral integrations at *Evi-2*. In all cell lines examined, viral integration at *Evi-2* resulted in the production of only truncated *Nf1* transcripts and no stable, full-length neurofibromin. Although neurofibromin is a GTPase-activating protein (GAP) for $p21^{ras}$ proteins, its loss in the BXH-2 leukemic cell lines was not correlated with an increased steady-state level of $p21^{ras}$ bound to GTP. These data suggest that neurofibromin is not the sole mediator of Ras-GAP activity in myeloid cells and may have a GAP-independent function in myeloid cells.

BXH-2 mice have one of the highest spontaneous incidences of retrovirally induced myeloid leukemias of any inbred mouse strain (7, 29). In an attempt to identify genes that cause myeloid disease in BXH-2 mice, we have been cloning somatically acquired proviruses from BXH-2 tumors and determining if they are located at common viral integration sites. One such common viral integration site that we identified is *Evi-2* (ecotropic viral integration site 2) (12). Approximately 15% of BXH-2 myeloid leukemias have viral integrations at *Evi-2* (12). The viral integrations at *Evi-2* are spread over an ~18-kb region and are all located within a single large intron of the neurofibromatosis type 1 (*Nf1*) gene (12, 14, 60).

The *Nf1* gene spans more than 350 kb of genomic DNA and encodes an mRNA of 12 to 13 kb comprising more than 50 exons (reviewed in reference 23). *Nf1* is expressed beginning early in development, and *Nf1* transcripts are found in many embryonic and adult tissues (13, 60, 62). The *Nf1*-encoded protein, neurofibromin, is 2,818 amino acids in length and shares a central region of homology with several GTPase-activating proteins (GAPs) (13, 64). GAP genes negatively regulate Ras by catalyzing the conversion of the active GTP-bound form of Ras to the inactive GDP-bound form (reviewed in reference 42).

One of the most common human genetic diseases, von Recklinghausen neurofibromatosis or neurofibromatosis type 1 (NF1), is caused by mutations in the *NF1* gene (60, 62). The two most common clinical features of NF1 include the formation of neurofibromas, which are benign tumors of the peripheral nerves composed mainly of Schwann cells and fibroblasts, and café-au-lait spots, which are hyperpigmented spots on the skin (23). While NF1 is inherited as an autosomal dominant disease, *NF1* mutations are recessive at the cellular level (23). *NF1* is thus a member of an ever-expanding class of genes, called tumor suppressor genes, in which both alleles must be mutated for tumor formation to occur. The tumor suppressor function of *NF1* is consistent with its postulated role as a negative regulator of Ras.

NF1 patients are at increased risk for developing certain malignancies, including neurofibrosarcomas, astrocytomas, pheochromocytomas, and embryonal rhabdomyosarcomas (2). Juvenile patients with NF1 also have an increased incidence of myeloid leukemia, notably juvenile chronic myelogenous leukemia and monosomy 7 syndrome (2, 3, 55). Leukemic cells from affected children with NF1 frequently show loss of heterozygosity for markers within and near the *NF1* gene, with retention of the mutant *NF1* allele, inherited from the parent with NF1 (55). These results are consistent with the hypothesis that mutations in the *NF1* gene predispose people to the development of myeloid leukemia. A small percentage of aged mice, heterozygous for a germ line *Nf1* mutation, also develop myeloid leukemia with loss of the wild-type *Nf1* allele in the tumor, suggesting that mutations in the murine gene predispose mice to myeloid tumor development as well (28).

During the cloning of the *Nf1* gene, three other genes, *Evi-2A*, *Evi-2B*, and *Omgp*, that are located in the same large *Nf1* intron as the *Evi-2* common integration site were identified (12, 14, 60, 61). The direction of transcription of all three genes is opposite that of *Nf1* (14, 60, 61). *Omgp* encodes a known protein, oligodendrocyte-myelin glycoprotein (43). The *Evi-2A* and *Evi-2B* genes encode novel genes of unknown function. *Evi-2A* and *Evi-2B* are expressed in a number of different cell types, including myeloid cells, and both genes are located within the *Evi-2* locus (12, 14). This finding has led to specu-

* Corresponding author. Phone: (301) 846-1260. Fax: (301) 846-6666.

lation that viral integration at *Evi-2* alters expression of *Evi-2A* or *Evi-2B* and that it is this altered expression that predisposes mice to myeloid tumor development.

In studies described here, we have derived a series of BXH-2 myeloid leukemia cell lines with and without viral integrations at *Evi-2* and used them to determine whether viral integration at *Evi-2* disrupts *Nf1* expression. We have also determined whether disruption of *Nf1* in BXH-2 myeloid tumor cells leads to changes in Ras-GTP levels.

MATERIALS AND METHODS

Generation of BXH-2 myeloid leukemic cell lines. Primary tumor cells were plated in high-glucose glutamine-containing Dulbecco's modified Eagle's medium (BioWhittaker, Walkersville, Md.) supplemented with 10% fetal bovine serum (BioWhittaker), 10% NCTC 109 medium (Sigma, St. Louis, Mo.), 10^{-5} M β-mercaptoethanol, 100 U of insulin (Sigma), per ml, 1 mM sodium pyruvate (Gibco-BRL, Gaithersburg, Md.), 1 mM oxalacetic acid (Sigma), 0.1 mM nonessential amino acids (Gibco-BRL), 10 mM *N*-2-hydroxyethylpiperazine-*N*′-2-ethanesulfonic acid (HEPES) buffer (Sigma), and penicillin-streptomycin (Gibco-BRL). Tumor cells were plated at 2.5×10^5 to 5×10^5 cells per ml and fed biweekly.

Preparation and analysis of DNA and RNA. High-molecular-weight genomic DNA was prepared and analyzed by Southern blotting as described before (29). For "unblot" analysis, the procedure of Tsao et al. (59) was followed, with minor modifications. Ten micrograms of genomic DNA was separated on an 0.8% agarose gel, dried under vacuum for 1.5 h at 50°C, and hybridized for 4 h at 55°C in the following buffer: 6× SSPE (20× SSPE is 175.6 g of NaCl, 27.6 g of NaH_2PO_4, and 7.6 g of disodium EDTA per liter [pH 7.4]), 5× Denhardt's solution (50× Denhardt's solution is 1% [wt/vol] Ficoll-400, 1% [wt/vol] polyvinylpyrrolidone, and 1% [wt/vol] bovine serum albumin [BSA; fraction V; Sigma]), 0.5% (wt/vol) sodium dodecyl sulfate (SDS), 0.05% (wt/vol) sodium phosphate, and 10 mg of denatured salmon sperm DNA per ml. The probe used was a polynucleotide kinase (New England Biolabs, Beverly, Mass.)-labeled oligonucleotide probe (Δenv, 5′-GTCTTCAATGTTACAAGGGTGGTTTG-3′) specific for murine AIDS-related viruses (MRVs) (16). The unblot was washed to 1× SSC (1× SSC is 0.15 M NaCl plus 0.015 sodium citrate [pH 7.0]) at 55°C. Probes B, D, and E from the *Evi-2* locus have been described before (12). The *eco* probe is a 400-bp *Sma*I fragment derived from the *env* gene of pAKV623 (15). The Cκ probe, used to detect rearrangements of the immunoglobulin κ light-chain (*Igk*) genes in *Bam*HI- and *Eco*RI-digested genomic DNAs, was a 4.5-kb *Hin*dIII-to-*Bam*HI fragment from the BALB/c mouse *Igk* constant-region gene (41). The J_H probe, used to detect immunoglobulin heavy-chain (*Igh*) gene rearrangements in *Eco*RI-digested genomic DNAs, was a 6.0-kb *Xba*I fragment from plasmid pRI-JH, which spans the mouse *Igh* gene joining region (1). The Jβ1 and Jβ2 probes (34) and their use to detect T-cell receptor β-chain gene (*Tcrb*) rearrangements have been described before (45).

Poly(A)$^+$ RNA was isolated by the method of Badley et al. (4). The RNA was separated on a 0.8% agarose–formaldehyde gel and transferred to a Zetabind (AMF Cuno, Inc.) membrane. The blot was hybridized by the method of Church and Gilbert (17). Northern (RNA) blots were stripped by boiling for 20 min in 0.1× SSPE–0.5% SDS and then rinsing twice in 2× SSPE. The *Nf1*-5′ probe was a 550-bp PCR-generated probe including sequences from the *Nf1* GAP-related domain, which is upstream of the large intron that contains *Evi-2*. The *Nf1*-5′ probe was amplified by using two primers, 5′-GGTTACCACAAGGATCTC CAG-3′ and 5′-GCTTCATACGGTGAGACAATGG-3′, and random-primed mouse brain cDNA as a template. The *Nf1*-3′ probe, from sequences downstream of the large intron that contains *Evi-2*, was generated by PCR using primers and plasmid pmDV1 as described before (13). The glyceraldehyde phosphate dehydrogenase probe was a 1.3-kb *Pst*I fragment from the rat glyceraldehyde phosphate dehydrogenase gene (20). Double-stranded probes were labeled with [α-^{32}P]dCTP (Amersham Life Science, Arlington Heights, Ill.) by using a random-priming kit (Stratagene, La Jolla, Calif.).

Western blot (immunoblot) analysis. For Western blot analysis, cells were rinsed in ice-cold Tris-buffered saline (TBS; 137 mM NaCl, 20 mM EDTA [pH 8.0]) and lysed in ice-cold lysis buffer (TBS with 1% Nonidet P-40, 10% glycerol, 1 mM phenylmethylsulfonyl fluoride, 10 μg of aprotinin per ml, 1 μg of leupeptin per ml, and 0.5 mM sodium vanadate). The lysed cells were rocked for 15 min at 4°C, the nuclei were pelleted, and the cytoplasmic lysates were stored at −70°C. Lysates from 7.5×10^5 cells were separated on SDS–6% polyacrylamide gels by the method of Laemmli (35) and electrotransferred at 0.5 A to 0.45-μm-pore-size nitrocellulose blots (Schleicher & Schuell, Keene, N.H.) in transfer buffer (25 mM Tris base, 192 mM glycine, 20% methanol) at 4°C for 4 h. These blots were blocked for 1 h in 1% BSA (fraction V; Sigma)–phosphate-buffered saline (PBS), hybridized overnight at 4°C with 1 μg of affinity-purified, amino-terminal antineurofibromin antisera (18) per ml in a 10-mg/ml mixture of BSA-PBS with 0.05% Tween 20, washed three times for 15 min each time at room temperature in 0.1% Tween 20–TBS, hybridized for 1 h at room temperature in 0.1% Tween 20–TBS with a 1/20,000 dilution of peroxidase-conjugated goat anti-rabbit antibody (Amersham Life Science), and washed as before, and the bound secondary antibody was visualized by using a commercially available chemiluminescence kit (ECL kit; Amersham Life Science).

Cytochemistry and flow cytometry. Leukemic cells were analyzed cytochemically for nonspecific esterase, *n*-naphthyl chloroacetate esterase, and myeloperoxidase, using commercially available kits (Sigma). WEHI-3 cells (50) were used as a positive control for these strains. Flow cytometry was performed with fluorescein isothiocyanate (FITC)- or phycoerythrin (PE)-conjugated monoclonal antibodies. The following monoclonal antibodies were supplied by Pharmingen (San Diego, Calif.) and used at 1 μg/10^6 cells: CD3-FITC, B220-FITC, Mac-1-FITC, Gr-1-PE, Thy-1.2-FITC, Sca-1-PE, and c-Kit-FITC. Rabbit antiserum against murine CD34 was supplied by Larry Laskey (Genentech, South San Francisco, Calif.) and used at a 1:200 dilution. Secondary goat anti-rabbit-FITC was then used at a 1:80 dilution. Cells were stained with antibodies diluted into 2.0% BSA–PBS. All incubations were at 4°C for 15 min; cells were washed three times and fixed in 1% paraformaldehyde–2.0% BSA–PBS. Positive cells had fluorescence intensities at least 10 times above the background level. Background fluorescence intensities were determined by using isotype-matched FITC- or PE-conjugated antibodies. Cell line EL4 (47) and primary mouse thymocytes were used as positive controls for CD3, Thy-1.2, and Sca-1 staining. Cell lines 70/Z3 (48) and WEHI-231 (36) were used as positive controls for B220 staining. Cell lines M1 (27) and granulocyte/macrophage colony-stimulating factor (GM-CSF)-induced myeloid cell cultures from fetal livers were used as positive controls for Mac-1, CD34, and c-Kit staining. Cell line WEHI-3 (50) and GM-CSF-induced myeloid cell cultures from fetal livers were used as positive controls for Gr-1 staining.

In vivo Ras-GTP assays. The assays were performed with cells grown to about 75% maximal density (about 2×10^6 to 3×10^6/ml for myeloid leukemia cell lines), which were then switched to fresh medium containing 10% dialyzed fetal bovine serum (Gibco-BRL), Dulbecco's modified Eagle's medium phosphate-free (BioWhittaker), 3% NCTC 109 medium (Sigma), 10^{-5} M β-mercaptoethanol, 1 mM sodium pyruvate (Gibco-BRL), 1 mM oxalacetic acid (Sigma), 10 mM HEPES buffer (Sigma), and penicillin-streptomycin (Gibco-BRL), plated at 3×10^6 cells per ml in 3 ml, and labeled with $^{32}P_i$ at 0.35 mCi/ml (1 Ci = 37 GBq) for 3 to 6 h. In some assays, the medium was supplemented with more serum, insulin, or GM-CSF. Cell lysis, immunoprecipitation of p21^{ras} with monoclonal antibody Y13-259 (Oncogene Science, Uniondale, N.Y.), and chromatography of the solubilized nucleotides were performed as previously described (65). Quantification of the chromatograms was done with a Molecular Dynamics PhosphorImager: SF radioanalytic system or densitometric scanning, which gave similar results, and the results were normalized for phosphate content.

RESULTS

BXH-2 leukemic cell lines. BXH-2 leukemic cell lines are notoriously difficult to establish, and characterization of only one BXH-2 tumor cell line has been published to date (6). Of 78 primary BXH-2 myeloid leukemias that we placed in culture, 14 (18%) were successfully established in vitro. Among the cell lines established are those that grow slowly and only when in contact with a fibroblast-like feeder layer, derived from the original tumor mass (Fig. 1B). Other lines grow quickly in culture without a feeder layer (Fig. 1A). Most of the cell lines are density dependent and have low plating efficiencies. Several of the cell lines grow faster when GM-CSF or interleukin-3 is added to the media, but none of the lines are dependent on these factors or insulin, which was routinely added to the media (data not shown).

Most of the cell lines have features consistent with a myelomonocytic origin. For example, eight of nine lines characterized in detail were positive for nonspecific esterase, which marks cells of the granulocytic (neutrophil) and monocyte/macrophage lineages, while three of the lines were positive for *n*-napthyl chloroacetate esterase, which marks cells of the granulocytic lineage (Table 1). None of the lines were positive for myeloperoxidase (MPO), which is expressed in more differentiated granulocytes and monocytes (37). Two of the lines had *Igh* rearrangements, which are sometimes seen in myeloid leukemia (52), and none had *Igk* or *Tcrb* rearrangements (Table 1), which are specific for B and T cells, respectively.

To further define the phenotypes of the cell lines, we stained the cells with fluorescently labeled antibodies specific for various cell surface antigens and analyzed them by flow cytometry (Table 2). With the exception of B140, which stained positive for the B-cell marker B220, none of the lines were positive for

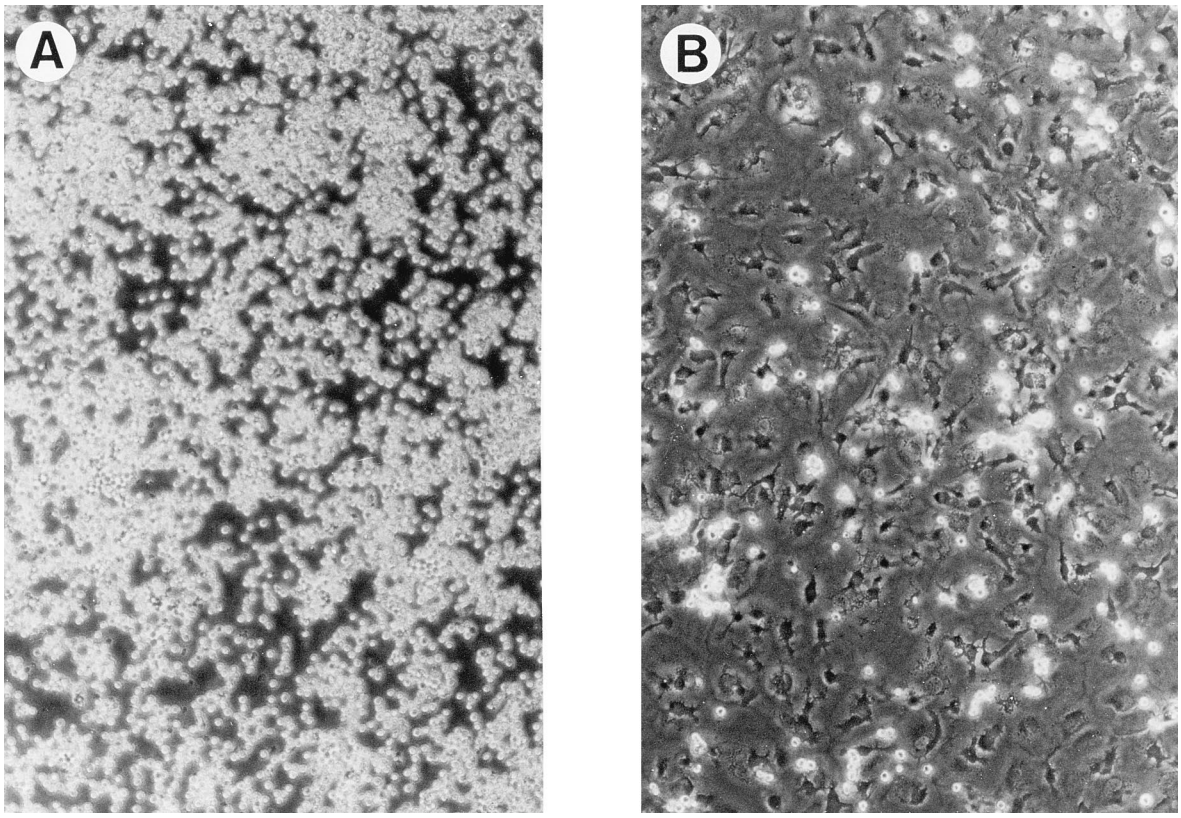

FIG. 1. Photomicrographs of BXH-2 leukemic cell lines in culture. (A) Cell line B117, which grows quickly as nonadherent, blast-like cells; (B) cell line B114, which grows slowly and only when in contact with a fibroblast-like, tumor-derived feeder layer. Magnification, ×100.

B220 or the T-cell marker CD3 (25). In contrast, most of the lines were positive for the myeloid lineage marker Mac-1 (25). Line B114 was also positive for the macrophage and granulocyte marker Gr-1 (25). The cell lines also variably expressed markers often found on immature or progenitor hematopoietic cells. These markers include Sca-1, CD34, c-Kit, and Thy-1.2 (9, 25, 44, 56). However, with the exception of CD34, only a small percentage of the cells growing in culture were positive for these markers. CD34 is a marker of immature murine hematopoietic cells, including the CFU-granulocyte/macrophage and CFU-spleen, but is not myeloid specific (33). CD34 is, however, usually expressed by human acute myeloid leukemia cells, which helps distinguish them from acute lymphoid leukemia (57). One cell line, B119, did not stain positive for any of the markers and may represent a primitive stem cell line which has lost CD34 expression as a secondary consequence of transformation or growth in culture.

BXH-2 leukemic cell lines harbor somatically acquired ecotropic and MRV proviruses. To determine if the cell lines harbor somatically acquired ecotropic proviruses, as expected by their postulated mode of retroviral induction, genomic DNA from each cell line was cleaved with *Pvu*II and analyzed

TABLE 1. Characteristics of BXH-2 leukemic cell lines

Line	Growth	Cytochemistry[a]			Gene rearrangements[b]				No. of proviruses[c]	
		NSE	CAE	MPO	*Igh*	*Igk*	*Tcrb*	*Evi-2*	Ecotropic	MRV
B106E	Slow	+	−	−	+	−	−	−	4	0
B106L	Fast	+	−	−	+	−	−	+	2	0
B112	Fast	+	+	−	−	−	−	−	1	0
B113	Fast	+	−	−	−	−	−	−	3	0
B114	Slow	+	+	−	−	−	−	+	2	0
B117	Fast	+	+	−	−	−	−	+	6	1
B119	Fast	+	−	−	+	−	−	−	2	0
B132	Fast	+	−	−	−	−	−	−	7	1
B139	Fast	+	−	−	−	−	−	−	2	1
B140	Fast	−	−	−	−	−	−	−	2	0

[a] Cells were stained for the myeloid esterases nonspecific esterase (NSE), *n*-naphthyl chloroacetate esterase (CAE), and myeloperoxidase (MPO). +, positive staining; −, negative staining.

[b] +, one or more DNA rearrangements were detected at the locus; −, no DNA rearrangements were detected.

[c] Number of somatically acquired ecotropic or MRV proviruses.

TABLE 2. Immunophenotypes of BXH-2 leukemic cell lines

Cell line	Phenotype[a]							
	CD3	B220	Mac-1	Gr-1	Thy-1.2	Sca-1	CD34	c-Kit
B106E	−	−	+	−	−	+/−	++	−
B106L	−	−	+	−	−	−	++	+/−
B112	−	−	+	−	+/−	−	++	+/−
B113	−	−	+/−	−	+/−	+/−	++	−
B114	−	−	++	++	−	++	−	+/−
B117	−	−	+	−	−	−	++	+/−
B119	−	−	−	−	−	−	−	−
B132	−	−	+	−	−	+/−	++	+/−
B139	−	−	++	−	−	−	+	+/−
B140	−	++	−	−	−	−	−	+/−

[a] −, 0% positive; +/−, 5 to 10% positive; +, 100% positive, dull; ++, 100% positive, bright.

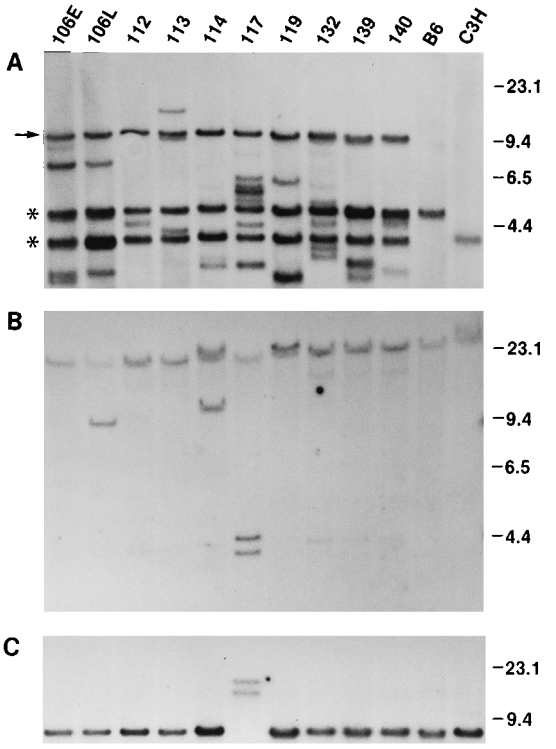

FIG. 2. Somatic acquisition of ecotropic proviruses and alterations at the *Evi-2* locus in BXH-2 leukemic cell lines. High-molecular-weight genomic DNA from BXH-2 cell lines (106E to 140) and the spleens of C57BL/6J (B6) and C3H/HeJ (C3H) mice were analyzed. (A) DNAs were digested with *Pvu*II and hybridized with an *env* probe specific for ecotropic proviruses (15). Two endogenous (i.e., germ line) ecotropic *Pvu*II proviral/cell DNA junction fragments, marked by asterisks, are seen in all BXH-2 DNAs. These represent *Emv1* and *Emv2*, which were inherited from the C3H/HeJ and C57BL/6J parental strains, respectively (29). In addition, these BXH-2 mice harbor a new endogenous, ecotropic virus whose 9.5-kb *Pvu*II proviral/cell DNA junction fragment is marked by an arrow. All of the cell lines have one or more additional, somatically acquired ecotropic proviruses, as evidenced by additional *Pvu*II proviral/cell DNA junction fragments. (B) DNA rearrangements at the *Evi-2* locus are detected by digestion of the DNAs with *Kpn*I and hybridization with *Evi-2* locus probe D (see Fig. 4). The germ line *Kpn*I fragment is 24.2 kb. The apparent doublets of this band in cell lines B114 and B119 are due to incomplete digestion. Alterations are seen in one allele of B114 and B106L cells. Cell line B117 has proviruses integrated into both alleles. As the D probe overlaps the site of proviral integration, four fragments are produced (see Fig. 4). The two large *Kpn*I fragments from B117 comigrate near 20 kb. The faint bands seen in lanes 132, 139, and 140 are not seen consistently and seem to be the result of nonspecific hybridization sometimes seen with probe D. (C) The DNAs were digested with *Eco*RI and hybridized with *Evi-2* locus probe B (see Fig. 4). Cell line B117 has one full-length and one smaller provirus integrated within this *Eco*RI fragment; one provirus has been integrated into each allele. Consistent with this notion, no germ line *Eco*RI fragment is seen in B117 DNA. The sizes (in kilobase pairs) and migration positions of molecular weight markers are shown at the right.

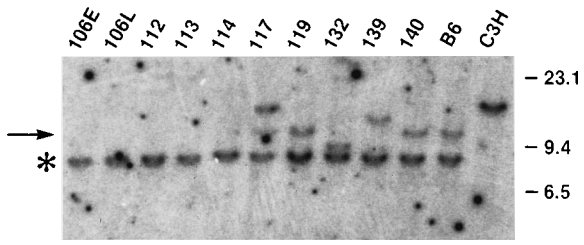

FIG. 3. Somatic acquisition of MRV proviruses in BXH-2 leukemic cell lines. Ten-microgram samples of genomic DNA from the cell lines (B106E to B140), male C57BL/6J (B6) mice, and female C3H/HeJ (C3H) mice were digested with *Eco*RI, separated on an 0.8% agarose gel, dried, and hybridized with an MRV-specific oligonucleotide probe, called Δenv (16), by the unblot procedure. *Eco*RI does not cleave within the MRV genome, and so each band represents a unique integrated provirus. The asterisk marks the position of the endogenous, or germ line, MRV-1 locus, present in BXH-2 mice, which was inherited from the C57BL/6J parental strain (16). An arrow marks the position of the germ line MRV-5 locus, which is located on the BXH-2 Y chromosome (16). Separate hybridization experiments with the *Zfy-2* probe, specific for the Y chromosome (39), shows that only B117, B119, and B140 are male cell lines (data not shown), consistent with the detection of an MRV-4-comigrating *Eco*RI band in these samples. Cell lines B117, B132, and B139 harbor one additional, somatically acquired MRV provirus.

by Southern blot hybridization using an ecotropic virus-specific envelope (*env*) probe (15). In such an analysis, each provirus generates a single 3′ provirus/cell junction fragment that is detectable with the ecotropic virus *env* probe. As seen in Fig. 2A, all cell lines harbor somatically acquired ecotropic proviruses. The number of somatically acquired proviruses ranged from 1 to 7 per line, with an average of 3.1 proviruses per line (Fig. 2A; Table 1). On the basis of their hybridization intensities, some of the proviruses appear to be present at less than one copy per cell. This result suggests that some of the tumors were oligoclonal or that additional proviruses are being acquired in culture. For cell line B106, it appears that the original tumor was oligoclonal, as early-passage B106 (B106E) cells harbor at least four somatically acquired ecotropic proviruses whereas late-passage B106 (B106L) cells harbor only a subset of these proviruses (Fig. 2A).

Approximately half of the somatically acquired proviruses previously characterized at *Evi-2* represent defective, nonecotropic proviruses (12, 16). This defective provirus contains two large deletions, one in *pol* and one in *env*, and is structurally related to another defective provirus, the murine AIDS virus (16). This defective virus has been termed MRV (16). Oligonucleotide probes that span the *pol* and *env* deletions in MRV are MRV specific and can be used to screen for the presence of somatically acquired MRV proviruses in tumor DNA. As seen in Fig. 3, three of the lines harbor somatically acquired MRV proviruses. In each case, only one somatically acquired MRV was detected per tumor (Fig. 3; Table 1).

Proviral integrations at *Evi-2* in BXH-2 leukemic cell lines. Two of the cell lines, B114 and B117, harbor proviral integrations at *Evi-2* (Fig. 2B). The position and type (ecotropic virus or MRV) of provirus integrated at *Evi-2* were determined by Southern blot analysis following digestion with *Kpn*I, which cuts once within each ecotropic and MRV proviral long terminal repeat, or *Eco*RI, which does not cleave ecotropic or MRV proviruses, and hybridization with *Evi-2* probes B, D, and E (Fig. 4) (12). The orientation of each provirus at *Evi-2* was determined by Southern blot analysis following digestion with *Sac*I or *Xba*I, which both cut asymmetrically within ecotropic and MRV proviruses. From the analysis shown in Fig. 2, it is apparent that line B117 has proviruses integrated in both *Evi-2* alleles. This is most easily observed in *Eco*RI-cleaved DNA (Fig. 2C). Instead of a normal 7.2-kb fragment, indicative of an unrearranged *Evi-2* allele, two fragments of 12.5 and 16.1 kb were observed. Both integrations are within the second exon of *Evi-2A*; one provirus is a full-length ecotropic provirus, and the other is an MRV provirus (Fig. 4). B114 has one full-length ecotropic provirus integrated just downstream of the second *Evi-2B* exon. The transcriptional orientation of all three of these proviruses is the same as that of *Evi-2A* and *Evi-2B* but opposite that of *Nf1* (Fig. 4).

The B106 cell line acquired a rearrangement at *Evi-2* during in vitro culture; therefore, B106L cells show the rearrangement, but B106E cells do not (Fig. 2A and B). It is possible that a minor population of cells with this rearrangement was

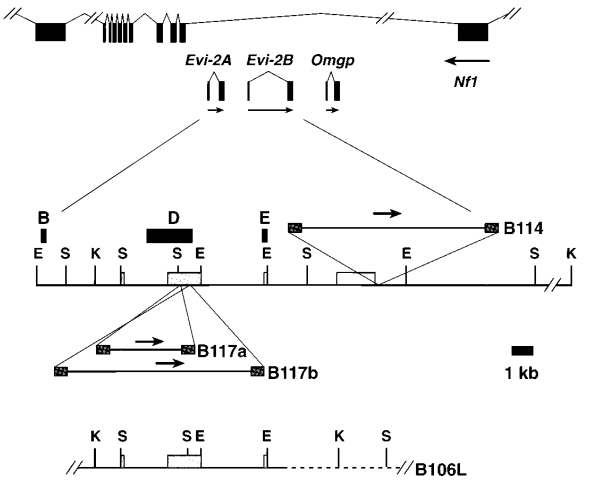

FIG. 4. Alterations at the *Evi-2* locus in BXH-2 leukemic cell lines. The upper part of the diagram shows (as black boxes) the relative positions, sizes, and orientations of exons from the *Evi-2A*, *Evi-2B*, *Omgp*, and *Nf1* genes, near the *Evi-2* locus. The lower part displays a restriction map of the *Evi-2* locus that includes the positions of exons from the *Evi-2A* gene (shown as hatched boxes) and the *Evi-2B* gene (shown as empty boxes). The following restriction enzyme sites are shown: *Eco*RI (E), *Sac*I (S), and *Kpn*I (K). The distance between the rightmost *Sac*I and *Kpn*I sites is 5.2 kb. *Evi-2* locus probes B, D, and E, described originally by Buchberg et al. (12), are shown above the restriction enzyme map as black boxes. The positions, sizes, and orientations of proviruses integrated at *Evi-2* in cell lines B114 and both alleles of B117 (B117a and B117b) are indicated. The position of the alteration at the *Evi-2* locus, in B106L cells, is shown at the bottom. The restriction map of *Evi-2* in B106L cells diverges (indicated by a dotted line) somewhere between the *Eco*RI and *Sac*I sites in the intron of the *Evi-2B* gene. Some of the data used to generate this figure were presented in references 12 and 14.

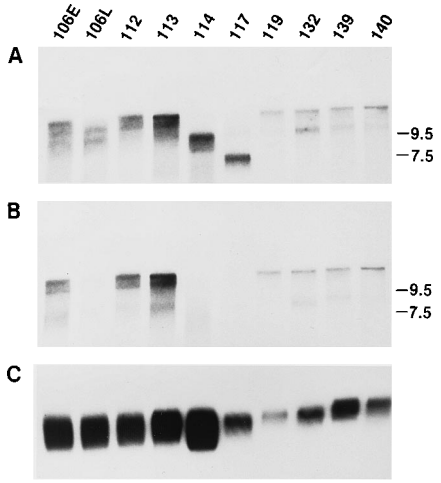

FIG. 5. *Nf1* transcripts expressed in BXH-2 leukemic cell lines. Poly(A)$^+$ RNA from the cell lines was fractionated on a 0.8% agarose–formaldehyde gel and blotted. (A) The blot was hybridized with a probe (*Nf1*-5′) from *Nf1* coding sequences upstream of the large intron that contains *Evi-2*. (B) The same blot was stripped and rehybridized with a probe (*Nf1*-3′) from *Nf1* coding sequences downstream of the large intron that contains *Evi-2*. (C) Differences in RNA loading were revealed by hybridization of the same blot with a rat glyceraldehyde phosphate dehydrogenase probe. The size (in kilobases) and migration positions of RNA molecular weight markers are indicated at the right.

present in the original tumor and selected during in vitro growth, or this rearrangement may have occurred de novo during in vitro passage of the tumor cells. Southern blot data are inconsistent with the presence of an ecotropic or MRV provirus at *Evi-2* in B106L cells. The precise nature of this rearrangement is under investigation.

***Nf1* mRNA expression in BXH-2 leukemic cell lines.** To determine if viral integrations at *Evi-2* affect *Nf1* expression, we performed a series of Northern blot analyses using poly(A)$^+$ RNA isolated from the BXH-2 leukemic cell lines (Fig. 5). Two hybridization probes were used in this analysis. One probe (*Nf1*-5′) was derived from *Nf1* coding sequences located upstream of *Evi-2*, while the second probe (*Nf1*-3′) was derived from *Nf1* coding sequences located downstream of *Evi-2*. All cells lines without viral integrations or rearrangements at *Evi-2* expressed a 12.5-kb transcript indicative of a full-length *Nf1* message (Fig. 5). A number of smaller transcripts were also expressed by these cell lines. While the exact nature of these smaller transcripts is not known, their variability in size and abundance in different RNA preparations suggests that they represent *Nf1* degradation products (Fig. 5 and data not shown).

B117 cells, which harbor viral integrations in both *Evi-2* alleles, produce no detectable wild-type *Nf1* transcripts (Fig. 5). In B117 cells, a truncated 7.4-kb transcript was detected with the upstream *Nf1*-5′ probe (Fig. 5A) but not the downstream *Nf1*-3′ probe (Fig. 5B), consistent with the notion that this transcript terminates within the viral sequences located at *Evi-2*. Likewise, in B114 cells, no normal *Nf1* transcript was detected. Instead, we identified a 9.0-kb transcript which, as in B117 cells, was detected only with the *Nf1*-5′ probe (Fig. 5A and B). This result was somewhat surprising since B114 cells harbor a single viral integration at *Evi-2*. This result is not, however, inconsistent with what would be expected for a tumor suppressor gene, in which both alleles must be mutated for tumor formation to occur. It is possible that B114 cells harbor a viral integration in the second *Nf1* allele that maps outside the *Evi-2* locus. This seems unlikely, however, since analysis of 153 BXH-2 tumors with cDNA probes representing most of the human *NF1* coding region identified only one tumor with a viral integration that mapped outside of the *Evi-2* locus (14a). It is thus likely that the second *Nf1* allele in B114 carries a mutation that was nonvirally induced.

B106L cells also produce very little, if any, normal *Nf1* transcripts although though they too appear to carry one normal *Evi-2* allele (Fig. 2). As expected, B106E cells, which do not harbor rearrangements at *Evi-2*, express wild-type *Nf1* transcripts (Fig. 5). The selection of cells in culture that fail to express neurofibromin suggests that *Nf1* loss may produce a selective growth advantage in vitro.

To determine if the truncated *Nf1* transcripts seen in B114 and B117 cells terminate within the viral sequences located at *Evi-2*, we hybridized the Northern blot shown in Fig. 5 with probes specific for MRV and ecotropic viruses. A message of the same size as the truncated *Nf1* transcript seen in B117 cells was detected with an MRV probe (data not shown), suggesting that this message represents a fusion between *Nf1* and MRV sequences. As the truncated transcript produced by B114 cells is the same size as the full-length ecotropic virus transcript, it was not possible to tell if this message is a fusion between *Nf1* and ecotropic viral sequences.

Neurofibromin expression in BXH-2 leukemic cell lines. To determine if truncated *Nf1* transcripts encode stable truncated protein, we performed Western blot analyses on lysates from the cell lines, using antisera that were directed against the amino-terminal third of neurofibromin (18) (Fig. 6). As expected, cells lines that lacked viral integrations at *Evi-2* expressed neurofibromin. Two of the lines, B106L and B117, which fail to express full-length *Nf1* transcripts, did not express any detectable neurofibromin, suggesting that these truncated proteins are unstable (Fig. 6). In contrast, B114 cells express

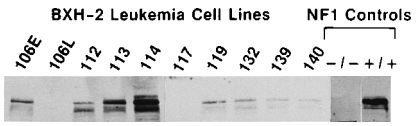

FIG. 6. Neurofibromin expression in BXH-2 leukemic cell lines. Lysates from 7.5×10^5 BXH-2 leukemic cells (B106E to B140), fetal liver cells of an embryo that carries two germ line null mutations at the *Nf1* gene (−/−; see reference 11), or fetal liver cells of a homozygous wild-type littermate (+/+) were loaded in the lanes. The lysates were separated on an SDS–0.6% polyacrylamide gel, blotted, and hybridized with antisera specific for the amino-terminal third of neurofibromin (18). Cell lines B117 and B106L fail to produce detectable levels of full-length neurofibromin, which we estimated to be about 250 kDa. Cell line B114 expresses an immunoreactive protein larger than that seen in any of the other samples.

multiple antineurofibromin-reactive proteins, both larger and smaller than wild-type neurofibromin (Fig. 6 and data not shown). As B114 cells produce only truncated *Nf1* mRNA (Fig. 5A), it is likely that these proteins represent alternative translation products of a mutant *Nf1*/provirus fusion transcript. These results are consistent with what has been observed in humans, in whom *NF1* mutations often lead to *NF1* mRNA or protein instability (5, 23, 31).

Ras-GTP levels in BXH-2 leukemic cell lines. To determine if neurofibromin loss in BXH-2 leukemic cells results in increased Ras-GTP levels, we metabolically labeled cells from each cell line with $^{32}P_i$, immunoprecipitated Ras proteins with the pan-Ras monoclonal antibody 13-259 (21), and separated the bound GDP and GTP on thin-layer chromatography plates (Fig. 7). As controls, we used NIH 3T3 cells, which have a low (about 5%) steady-state level of Ras-GTP (19, 30, 31), and v-*ras*-transformed NIH 3T3 cells, called 1423 cells (19, 31). v-*ras* is insensitive to GAP activity, and cells expressing v-*ras* at high levels have Ras-GTP levels approaching 50%, the level expected for cells lacking GAP activity (10, 19, 30, 42). About 5 to 10% of Ras proteins were bound to GTP in all of the BXH-2 leukemic cell lines tested (Fig. 7; Table 3). More importantly, in a given assay, there was never a significant difference between lines that express neurofibromin and those that do not (Fig. 7; compare B106E with B106L).

TABLE 3. Ras-GTP levels in BXH-2 leukemic cell lines

Cell line	Neurofibromin[a]	% Ras-GTP[b] (avg ± SD)
NIH 3T3	+	5.9 ± 0.9
1423[c]	+	47.3 ± 8.4
B106E	+	4.4 ± 2.2
B106L	−	3.0 ± 1.1
B112	+	3.9 ± 1.1
B113	+	4.9 ± 1.2
B114	+[d]	8.8
B117	−	8.9 ± 4.0
B119	+	4.9
B132	+	ND
B139	+	13.4 ± 1.5
B140	+	ND

[a] Western blot detection (+) or lack of detection (−) of neurofibromin.
[b] Percentage of total cellular p21^{ras} protein bound to GTP. Experiments for B114 and B119 were carried out only once. Experiments for B139 were done twice, and those for all other cell lines were done three or more times. ND, not determined.
[c] A v-*ras* transformant of NIH 3T3 cells used as a positive control for deregulated Ras-GAP activity.
[d] Cell line B114 produces a truncated *Nf1* transcript and several altered neurofibromin forms.

DISCUSSION

As part of our effort to determine whether viral integration at *Evi-2* predisposes mice to myeloid disease by disrupting expression of *Nf1*, we have established a number of BXH-2 tumor cell lines, with and without proviral integrations at *Evi-2*, and used them to determine whether proviral integration at *Evi-2* disrupts *Nf1* expression. The results of these studies are consistent with the hypothesis that proviral disruption of *Nf1* expression is causally associated with myeloid tumor development. In three BXH-2 cells lines that harbor *Evi-2* rearrangements, only truncated *Nf1* transcripts are produced. Truncated transcripts appear to result from premature termination of *Nf1* transcripts within viral sequences located at *Evi-2*. In addition, two of the cell lines expressing truncated *Nf1* transcripts produced no detectable neurofibromin. This result is consistent with what has been observed for human *NF1* mutations, which often lead to mRNA or protein instability (5, 19, 23, 31).

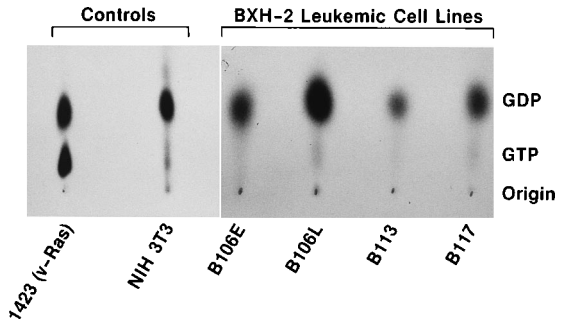

FIG. 7. In vivo p21^{ras}-GTP assay of four BXH-2 leukemic cell lines. The figure depicts a typical result for this assay with 1423 cells, which express v-*ras* at high levels, and with NIH 3T3, B106E, B106L, B113, and B117 cells. The B106E and B113 lines express neurofibromin, while the B106L and B117 lines do not. The origin and the migration positions of GTP and GDP on the thin-layer chromatogram are indicated at the right. The 1423 and NIH 3T3 cells served as controls for high and low Ras-GTP levels, respectively.

Two other findings reported here also support the notion that *Nf1* mutations induce myeloid tumor development. First, one BXH-2 tumor cell line that we established has viral integrations in both *Evi-2* alleles (Fig. 2). This pattern of biallelic integration is rare for common viral integration sites that harbor dominantly acting oncogenes but would be expected for a common viral integration site harboring a tumor suppressor gene. Second, two of the BXH-2 tumor cell lines with viral integrations at *Evi-2* express only truncated *Nf1* transcripts despite the fact that both contain a viral integration in only one *Evi-2* allele. These results suggest that the second *Evi-2* allele in each cell line carries a nonvirally induced mutation, perhaps a small deletion or point mutation, that results in the production of an unstable *Nf1* message. Again, this result would be expected for a tumor suppressor gene.

Another tumor suppresser gene, *p53*, has also been shown to be inactivated by virus integration in Friend murine leukemia virus-induced erythroleukemias (8, 24). As with *Nf1*, inactivation of the second *p53* allele can occur by a nonviral mechanism or by integration of a second provirus.

The identification of two genes, *Evi-2A* and *Evi-2B*, that are located near *Evi-2* led to the speculation that viral integration at *Evi-2* alters expression of one of these genes and that it is this altered expression, not disruption of *Nf1*, that predisposes mice to myeloid disease. However, in addition to the results described above, a number of other findings suggest this is not the case. For example, one of the BXH-2 cell lines, B117,

carries viral integrations in both *Evi-2A* alleles, and no normal *Evi-2A* transcripts are expressed (data not shown). However, other BXH-2 cell lines (i.e., B114) harbor viral integrations located outside *Evi-2A*, and normal levels of *Evi-2A* transcripts are expressed (data not shown). Similarly, consistent changes in *Evi-2B* expression were not observed in any of the BXH-2 cell lines described here (data not shown). The presence of viral integrations that appear to be activating in some cell lines but inactivating in others would seem inconsistent with the involvement of *Evi-2A* and *Evi-2B* in myeloid tumor induction.

If *Nf1* mutations are responsible for myeloid tumor induction, why are proviruses clustered at *Evi-2* when viral integration at many other sites in the *Nf1* gene could inactivate *Nf1* expression? While the answer to this question is not known, we speculate that *Evi-2* is a hot spot for viral integration. Perhaps the chromatin is more open at this site as a result of active transcription of *Evi-2A* and *Evi-2B*, which are expressed in myeloid cells (12, 14). Indirect evidence suggests that proviral integration favors regions within or near actively transcribed genes (54).

ras deregulation seems to be a common event in myeloid tumor induction (reviewed in reference 53). For example, *ras* point mutations have been identified in 30 to 50% of human acute myeloid leukemia and myelodysplastic syndromes (38, 46). *ras* point mutations are also found in juvenile chronic myelogenous leukemia patients without underlying NF1 disease (32). However, *ras* point mutations are not detected in juvenile chronic myelogenous leukemia patients with NF1 syndrome, suggesting that *NF1* gene loss and *ras* point mutations are functionally equivalent (32). Likewise, the Bcr-Abl fusion protein, produced by the t(9;22) translocation chromosome in adult chronic myelogenous leukemia, has been shown to interact with the adapter molecule Grb2, which binds the GDP-GTP exchanger Sos2 (49). Activated Sos2, in turn, activates Ras by promoting exchange of GTP for GDP.

The findings presented above suggest that *Nf1* gene loss might lead to increased Ras-GTP levels in cells. Indeed, increased Ras-GTP levels have been observed in neurofibrosarcoma cell lines that fail to express neurofibromin (5, 19). Melanomas and neuroblastomas that also fail to express neurofibromin do not, however, show significantly increased Ras-GTP levels (31, 58). This finding has led to the speculation that *Nf1* may also function as a downstream effector molecule of *ras* and that this function may be cell type specific. It has also been suggested that *Nf1* may have *ras*-independent functions. This suggestion is based on the finding that *Nf1* overexpression inhibits growth of normal and v-*ras*-transformed NIH 3T3 cells and that v-*ras* is insensitive to the GAP activity of neurofibromin (30).

As others have reported for melanomas and neuroblastomas (31, 58), we found no significant differences in the steady-state Ras-GTP levels between myeloid leukemic cell lines that express neurofibromin and those that do not. This was true no matter what conditions were used to grow the cell lines, including high or low fetal bovine serum and with or without the addition of GM-CSF (data not shown). It is possible that in myeloid cells, neurofibromin does not significantly affect Ras-GTP levels but competes with Ras effector molecules, such as Raf, for binding to Ras-GTP. This hypothesis is consistent with the rather weak Ras-GAP activity of neurofibromin compared with the activity of $p120^{GAP}$ (40), the high affinity of neurofibromin for Ras-GTP (40), and the fact that neurofibromin and Raf cannot simultaneously bind to Ras-GTP (63). Alternatively, neurofibromin may regulate other Ras family members in myeloid cells. For example, the neurofibromin GAP-related domain binds to the R-Ras protein and activates its GTPase activity (51).

It is likely that *Nf1* mutations alone are not sufficient to induce acute myeloid disease such as that observed in BXH-2 mice. For example, deletions of one copy of chromosome 7, or 7q deletions, are frequently seen in myeloid leukemias that develop in patients with NF1 disease (22, 55). It is generally assumed that chromosome 7 carries a tumor suppressor gene that is important for myeloid tumor progression. The concordance of phenotype (i.e., myelomonocytic leukemia) and gene involvement (i.e., *NF1*) between the NF1 syndrome-associated myeloid diseases and BXH-2 cell lines with *Evi-2* integrations is very striking and suggests that the BXH-2 cell lines produced in these studies should provide useful reagents for identifying genes that cooperate with *NF1* to induce acute disease. On average, each BXH-2 cell line carries three somatic proviruses; some of these proviruses may be affecting the expression of genes that cooperate with *Nf1* to induce acute disease. Like *Evi-2*, these cooperating genes can be identified by cloning other somatic proviruses from these cell lines and determining if they are located in common viral integration sites.

Eighty-five percent of BXH-2 myeloid leukemias do not harbor viral integrations at *Evi-2*. It is possible that these cell lines harbor viral integrations in other cellular genes, the mutation of which can substitute for *Nf1* gene loss. Again, by identifying common integration sites in these tumors, it may be possible to identify these genes, which may include other genes in the *ras* pathway or other pathways that are functionally equivalent.

ACKNOWLEDGMENTS

This work was sponsored by the National Cancer Institute under contract N01-C0-46000 with ABL. D.A.L. is a Leukemia Society of America Fellow.

We thank Arthur Buchberg for the *Evi-2* locus probes, Cami Brannan for the *Nf1* gene probes, Nancy Ratner for the antineurofibromin antisera, and Larry Laskey (Genentech) for the rabbit antisera recognizing murine CD34. We also thank Jeffrey DeClue and Maureen Johnson for technical advice with the in vivo Ras-GTP assay and David Kaplan for technical advice with Western blot detection of neurofibromin. We acknowledge Louis Finch and the Clinical Service Flow Laboratory at the NCI-FCRDC for performing flow cytometric analyses. We also thank the members of the Mammalian Genetics Laboratory for critical review of the manuscript.

REFERENCES

1. **Alt, F., N. Rosenberg, S. Lewis, E. Thomas, and D. Baltimore.** 1981. Organization and reorganization of immunoglobulin genes in A-MuLV-transformed cells: rearrangement of heavy but not light chain genes. Cell **27:**381–390.
2. **Bader, J. L.** 1986. Neurofibromatosis and cancer. Ann. N.Y. Acad. Sci. **486:**56–65.
3. **Bader, J. L., and R. W. Miller.** 1978. Neurofibromatosis and childhood leukemia. J. Pediatr. **92:**925–929.
4. **Badley, J. E., G. A. Bishop, T. S. John, and J. A. Frelinger.** 1988. A simple, rapid method for the purification of poly A^+ RNA. BioTechniques **6:**114–116.
5. **Basu, T. N., D. H. Gutmann, J. A. Fletcher, T. W. Glover, F. S. Collins, and J. Downward.** 1992. Aberrant regulation of ras proteins in malignant tumor cells from type 1 neurofibromatosis patients. Nature (London) **356:**713–715.
6. **Bedigian, H. G., D. A. Johnson, N. A. Jenkins, N. G. Copeland, and R. Evans.** 1984. Spontaneous and induced leukemias of myeloid origin in recombinant inbred BXH-2 mice. J. Virol. **51:**586–594.
7. **Bedigian, H. G., B. A. Taylor, and H. Meier.** 1981. Expression of murine leukemia viruses in the highly lymphomatous BXH-2 recombinant inbred mouse strain. J. Virol. **39:**632–640.
8. **Ben David, Y., V. R. Prideaux, V. Chow, and S. Benchimol.** 1988. Inactivation of the *p53* oncogene by internal deletion or retroviral integration in erythroleukemic cell lines induced by Friend leukemia virus. Oncogene **3:**179–185.
9. **Berman, J. W., and R. S. Basch.** 1985. Thy-1 antigen expression by murine hematopoietic precursor cells. Exp. Hematol. **13:**1152–1156.
10. **Bourne, H. R., D. A. Sanders, and F. McCormick.** 1990. The GTPase superfamily: a conserved switch for diverse cell functions. Nature (London) **348:** 125–132.
11. **Brannan, C. I., A. S. Perkins, K. S. Vogel, N. Ratner, M. L. Nordlund, S. W. Reid, A. M. Buchberg, N. A. Jenkins, L. F. Parada, and N. G. Copeland.** 1994. Targeted disruption of the neurofibromatosis type-1 gene leads to developmental abnormalities in heart and various neural crest-derived tissues. Genes Dev. **8:**1019–1029.
12. **Buchberg, A. M., H. G. Bedigian, N. A. Jenkins, and N. G. Copeland.** 1990.

Evi-2, a common integration site involved in murine myeloid leukemogenesis. Mol. Cell. Biol. **10:**4658–4666.
13. **Buchberg, A. M., L. S. Cleveland, N. A. Jenkins, and N. G. Copeland.** 1990. Sequence homology shared by neurofibromatosis type-1 gene and *IRA-1* and *IRA-2* negative regulators of the RAS cyclic AMP pathway. Nature (London) **347:**291–294.
14. **Cawthon, R. M., L. B. Andersen, A. M. Buchberg, G. Xu, P. O'Connel, D. Viskochil, R. B. Weiss, M. R. Wallace, D. A. Marchuk, M. Culver, J. Stevens, N. A. Jenkins, N. G. Copeland, F. S. Collins, and R. White.** 1991. cDNA sequence and genomic structure of *EVI-2B*, a gene lying within an intron of the neurofibromatosis type 1 gene. Genomics **9:**446–460.
14a. **Ceci, J.** Unpublished data.
15. **Chattopadhyay, S. K., M. L. Lander, E. Rands, and D. R. Lowy.** 1980. Structure of endogenous murine leukemia virus DNA in mouse genomes. Proc. Natl. Acad. Sci. USA **77:**5774–5778.
16. **Cho, B., J. D. Shaughnessy, D. A. Largaespada, A. M. Buchberg, H. G. Bedigian, N. A. Jenkins, and N. G. Copeland.** Unpublished data.
17. **Church, G. M., and W. Gilbert.** 1984. Genomic sequencing. Proc. Natl. Acad. Sci. USA **81:**1991–1995.
18. **Daston, M. M., H. Scrable, M. Nordlund, A. K. Sturbaum, L. M. Nissen, and N. Ratner.** 1992. The protein product of the neurofibromatosis type 1 gene is expressed at highest abundance in neurons, Schwann cells, and oligodendrocytes. Neuron **8:**415–428.
19. **DeClue, J. E., A. G. Papageorge, J. A. Fletcher, S. R. Diehl, N. Ratner, W. C. Vass, and D. R. Lowy.** 1992. Abnormal regulation of mammalian $p21^{ras}$ contributes to malignant tumor growth in von Recklinghausen (type 1) neurofibromatosis. Cell **69:**265–273.
20. **Fort, P., L. Marty, M. Piechaczyk, S. E. Sabrouty, C. Dani, P. Jeanteur, and J. M. Blanchard.** 1985. Various rat adult tissues express only one major mRNA species from the glyceraldehyde-3-phosphate-dehydrogenase multigenic family. Nucleic Acids Res. **13:**1431–1442.
21. **Furth, M. E., L. J. Davis, B. Fleurdelys, and E. M. Scolnick.** 1982. Monoclonal antibodies to the p21 products of the transforming gene of Harvey murine sarcoma virus and of the cellular *ras* gene family. J. Virol. **43:**294–304.
22. **Ghione, F., C. Mecucci, M. Symann, J. Michaux, M. C.-V. Daele, and H. V. D. Berge.** 1986. Cytogenetic investigations in childhood chronic myelocytic leukemia. Cancer Genet. Cytogenet. **20:**317–323.
23. **Gutmann, D. H., and F. S. Collins.** 1993. The neurofibromatosis type 1 gene and its protein product, neurofibromin. Neuron **10:**335–343.
24. **Hicks, G. G., and M. Mowat.** 1988. Integration of Friend murine leukemia virus into both alleles of the *p53* oncogene in an erythroleukemic cell line. J. Virol. **62:**4752–4755.
25. **Holmes, K. L., and H. C. Morse III.** 1988. Murine hematopoietic cell surface antigen expression. Immunol. Today **9:**344–350.
26. **Huynh, D. P., T. Nechiporuk, and S. M. Pulst.** 1994. Differential expression and tissue distribution of type I and type II neurofibromins during mouse fetal development. Dev. Biol. **161:**538–551.
27. **Ihle, J. N., A. Rein, and R. Murral.** 1984. Immunologic and virologic mechanisms in retrovirus-induced murine leukemogenesis. Adv. Viral Oncol. **4:**95–135.
28. **Jacks, T., T. S. Shih, E. M. Schmitt, R. T. Bronson, A. Bernards, and R. A. Weinberg.** 1994. Tumor predisposition in mice heterozygous for a targeted mutation in *Nf1*. Nat. Genet. **7:**353–361.
29. **Jenkins, N. A., N. G. Copeland, B. A. Taylor, H. G. Bedigian, and B. K. Lee.** 1982. Ecotropic murine leukemia virus DNA content of normal and lymphomatous tissues of BXH-2 recombinant inbred mice. J. Virol. **42:**379–388.
30. **Johnson, M. R., J. E. DeClue, S. Felzmann, W. C. Vass, G. Xu, R. White, and D. R. Lowy.** 1994. Neurofibromin can inhibit Ras-dependent growth by a mechanism independent of its GTPase-accelerating function. Mol. Cell. Biol. **14:**641–645.
31. **Johnson, M. R., A. T. Look, J. E. DeClue, M. B. Valentine, and D. R. Lowy.** 1993. Inactivation of the *NF1* gene in human melanoma and neuroblastoma cell lines without impaired regulation of GTP-Ras. Proc. Natl. Acad. Sci. USA **90:**5539–5543.
32. **Klara, R., D. C. Paderanga, K. Olson, and K. M. Shannon.** 1994. Genetic analysis is consistent with the hypothesis that NF1 limits myeloid growth through $p21^{ras}$. Blood **84:**3435–3439.
33. **Krause, D. S., T. Ito, M. J. Fackler, O. M. Smith, M. I. Collector, S. J. Sharkis, and W. S. May.** 1994. Characterization of murine CD34, a marker for hematopoietic progenitor and stem cells. Blood **84:**691–701.
34. **Kronenberg, M., J. Governmann, R. Haars, M. Malissen, E. Kraig, L. Phillips, T. Pelovitch, M. Suciu-Foca, and L. Hood.** 1985. Rearrangements and transcripts of the β-chain genes of the T-cell antigen receptor in different types of murine lymphocytes. Nature (London) **313:**647–653.
35. **Laemmli, U. K.** 1978. Cleavage of structural proteins during the assembly of the head of bacteriophage T4. Nature (London) **227:**680–685.
36. **Lanier, L. L., and N. L. Warner.** 1981. Cell cycle related heterogeneity of Ia antigen expression on a murine B lymphoma cell line: Analysis by flow cytometry. J. Immunol. **126:**626–631.
37. **Lubbert, M., F. Herrmann, and H. P. Koeffler.** 1991. Expression and regulation of myeloid-specific genes in normal and leukemic myeloid cells. Blood **77:**909–924.
38. **Lubbert, M., G. Kitchingman, F. McCormick, R. Mertelsmann, F. Herrmann, and H. P. Koeffler.** 1992. Prevalence of N-ras mutations in children with myelodysplastic syndromes and acute myeloid leukemia. Oncogene **7:**263–268.
39. **Mardon, G., and D. C. Page.** 1989. The sex-determining region of the mouse Y chromosome encodes a protein with a highly acidic domain and 13 zinc fingers. Cell **56:**765–770.
40. **Martin, G. A., D. Viskochil, G. Bollag, P. C. McCabe, W. J. Crosier, H. Haubruck, L. Conroy, R. Clark, P. O'Connell, R. M. Cawthon, M. A. Innis, and F. McCormick.** 1990. The GAP-related domain of the neurofibromatosis type 1 gene product interacts with ras p21. Cell **63:**843–849.
41. **Max, E. E., J. G. Seidman, and P. Leder.** 1979. Sequences of five potential recombination sites encoded close to an immunoglobulin κ constant region gene. Proc. Natl. Acad. Sci. USA **76:**3450–3454.
42. **McCormick, F.** 1989. ras GTPase activating protein: signal transmitter and signal terminator. Cell **56:**5–8.
43. **Mikol, D. D., J. R. Gulcher, and K. Stefansson.** 1990. The oligodendrocyte-myelin glycoprotein belongs to a distinct family of proteins and contains the HNK-1 carbohydrate. J. Cell Biol. **110:**471–479.
44. **Miller, B. A., J. M. Lipton, D. C. Lynch, S. J. Burakoff, and D. G. Nathan.** 1985. THY-1 is a differentiation antigen that characterizes immature murine erythroid and myeloid hematopoietic progenitors. J. Cell. Physiol. **123:**25–32.
45. **Mucenski, M. L., B. A. Taylor, N. A. Jenkns, and N. G. Copeland.** 1986. AKXD recombinant inbred strains: models for studying the molecular genetic basis of murine lymphomas. Mol. Cell. Biol. **6:**4236–4243.
46. **Neubauer, A., K. Shannon, and E. Liu.** 1991. Mutation of the ras protooncogenes in childhood monosomy 7. Blood **77:**594–598.
47. **Old, L. J., E. A. Boyse, and E. Stockert.** 1965. The G(Gross) leukemia antigen. Cancer Res. **25:**813–819.
48. **Paige, C. J., P. W. Kincade, and P. Ralph.** 1978. Murine B cell leukemia line with inducible surface immunoglobulin expression. J. Immunol. **121:**641–647.
49. **Puil, L., J. Lui, G. Gish, G. Mbamalu, D. Bowtell, P. G. Pelicci, R. Arlinghaus, and T. Pawson.** 1994. Bcr-abl oncoproteins bind directly to activators of the ras signalling pathway. EMBO J. **13:**764–773.
50. **Ralph, P., and I. Nakoinz.** 1977. Direct toxic effects of immunopotentiators on monocytic, myelomonocytic, and histiocytic or macrophage tumor cells in culture. Cancer Res. **37:**546–550.
51. **Rey, I., P. Taylor-Harris, H. von Erp, and A. Hall.** 1994. R-ras interacts with rasGAP, neurofibromin and c-raf but does not regulate cell growth or differentiation. Oncogene **9:**685–692.
52. **Ru, M., C. Shustik, and E. Rassart.** 1993. Graffi murine leukemia virus: molecular cloning and characterization of the myeloid leukemia-inducing agent. J. Virol. **67:**4722–4731.
53. **Sawyers, C., and C. T. Denny.** 1994. Chronic myelomonocytic leukemia: tel-a-kinase what ets all about. Cell **77:**171–173.
54. **Scherdin, U., K. Rhodes, and M. Breindl.** 1990. Transcriptionally active genome regions are preferred targets for retrovirus integration. J. Virol. **64:**907–912.
55. **Shannon, K. M., P. O'Connell, G. A. Martin, D. Paderanga, K. Olson, P. Dinndorf, and F. McCormick.** 1994. Loss of the normal *NF1* allele from the bone marrow of children with type 1 neurofibromatosis and malignant myeloid disorders. N. Engl. J. Med. **330:**597–601.
56. **Spangrude, G. J., S. Heimfeld, and I. L. Weissman.** 1988. Purification and characterization of mouse hematopoietic stem cells. Science **241:**58–62.
57. **Sutherland, D. R., and A. Keating.** 1992. The CD34 antigen: structure, biology, and potential clinical applications. J. Hematother. **1:**115–129.
58. **The, I., A. E. Murthy, G. E. Hannigan, L. B. Jacoby, A. G. Menon, J. F. Gusella, and A. Bernards.** 1993. Neurofibromatosis type 1 gene mutations in neuroblastoma. Nat. Genet. **3:**62–66.
59. **Tsao, S. G. S., C. F. Brunk, and R. E. Pearlman.** 1983. Hybridization of nucleic acids directly in agarose gels. Anal. Biochem. **131:**365–372.
60. **Viskochil, D., A. M. Buchberg, G. Xu, R. M. Cawthon, J. Stevens, R. K. Wolff, M. Culver, J. C. Carey, N. G. Copeland, N. A. Jenkins, R. White, and P. O'Connell.** 1990. Deletions and a translocation interrupt a cloned gene at the neurofibromatosis type 1 locus. Cell **62:**187–192.
61. **Viskochil, D., R. Cawthon, P. O'Connell, G. Xu, J. Stevens, M. Culver, J. Carey, and R. White.** 1991. The gene encoding the oligodendrocyte-myelin glycoprotein is embedded within the neurofibromatosis type 1 gene. Mol. Cell. Biol. **11:**906–912.
62. **Wallace, M. R., D. A. Marchuk, L. B. Andersen, R. Letcher, H. M. Odeh, A. M. Saulino, J. W. Fountain, A. Brereton, J. Nicholson, A. L. Mithchell, B. H. Brownstein, and F. S. Collins.** 1990. Type 1 neurofibromatosis gene: identification of a large transcript disrupted in three NF1 patients. Science **249:**181–186.
63. **Warne, P. H., P. R. Vicana, and J. Downward.** 1993. Direct interaction of Ras and the amino-terminal region of Raf-1 *in vitro*. Nature (London) **364:**352–355.
64. **Xu, G., P. O'Connell, D. Viskochil, R. Cawthon, M. Robertson, M. Culver, D. Dunn, J. Stevens, R. Gesteland, R. White, and R. Weiss.** 1990. The neurofibromatosis type-1 gene encodes a protein related to GAP. Cell **62:**599–608.
65. **Zhang, K., A. G. Papageorge, and D. R. Lowy.** 1992. Mechanistic aspects of signalling through ras in NIH 3T3 cells. Science **257:**671–674.